

## RESEARCH ARTICLE

# Increased wood biomass growth is associated with lower wood density in *Quercus petraea* (Matt.) Liebl. saplings growing under elevated CO<sub>2</sub>

Janko Arsić<sup>1,2</sup>, Marko Stojanović<sup>1\*</sup>, Lucia Petrovičová<sup>1,2</sup>, Estelle Noyer<sup>1</sup>, Slobodan Milanović<sup>3,4</sup>, Jan Světlík<sup>1,2</sup>, Petr Horáček<sup>1,5</sup>, Jan Krejza<sup>1,2</sup>

**1** Global Change Research Institute of the Czech Academy of Sciences, Brno, Czech Republic, **2** Department of Forest Ecology, Faculty of Forestry and Wood Technology, Mendel University in Brno, Brno, Czech Republic, **3** Faculty of Forestry, University of Belgrade, Belgrade, Serbia, **4** Department of Forest Protection and Wildlife Management, Faculty of Forestry and Wood Technology, Mendel University in Brno, Brno, Czech Republic, **5** Department of Wood Science and Technology, Faculty of Forestry and Wood Technology, Mendel University in Brno, Brno, Czech Republic

\* [stojanovic.m@czechglobe.cz](mailto:stojanovic.m@czechglobe.cz)



## OPEN ACCESS

**Citation:** Arsić J, Stojanović M, Petrovičová L, Noyer E, Milanović S, Světlík J, et al. (2021) Increased wood biomass growth is associated with lower wood density in *Quercus petraea* (Matt.) Liebl. saplings growing under elevated CO<sub>2</sub>. PLoS ONE 16(10): e0259054. <https://doi.org/10.1371/journal.pone.0259054>

**Editor:** Fabricio José Pereira, Universidade Federal de Alfenas, BRAZIL

**Received:** June 17, 2021

**Accepted:** October 11, 2021

**Published:** October 22, 2021

**Copyright:** © 2021 Arsić et al. This is an open access article distributed under the terms of the [Creative Commons Attribution License](https://creativecommons.org/licenses/by/4.0/), which permits unrestricted use, distribution, and reproduction in any medium, provided the original author and source are credited.

**Data Availability Statement:** All relevant data are within the manuscript and its [Supporting information](#) files.

**Funding:** The work was supported by the Internal Grant Agency of Mendel University in Brno with grant number 030/2020, IGRÁČEK MENDELU project CZ.02.2.69/0.0/0.0/19\_073/0016670, reg. numb. SGC-2021-013 and Ministry of Education, Youth and Sports of CR within the CzeCOS program, grant number LM2018123. The funders

## Abstract

Atmospheric carbon dioxide (CO<sub>2</sub>) has increased substantially since the industrial revolution began, and physiological responses to elevated atmospheric CO<sub>2</sub> concentrations reportedly alter the biometry and wood structure of trees. Additionally, soil nutrient availability may play an important role in regulating these responses. Therefore, in this study, we grew 288 two-year-old saplings of sessile oak (*Quercus petraea* (Matt.) Liebl.) in lamellar glass domes for three years to evaluate the effects of CO<sub>2</sub> concentrations and nutrient supply on above- and belowground biomass, wood density, and wood structure. Elevated CO<sub>2</sub> increased above- and belowground biomass by 44.3% and 46.9%, respectively. However, under elevated CO<sub>2</sub> treatment, sapling wood density was markedly lower (approximately 1.7%), and notably wider growth rings—and larger, more efficient conduits leading to increased hydraulic conductance—were observed. Moreover, despite the vessels being larger in saplings under elevated CO<sub>2</sub>, the vessels were significantly fewer ( $p = 0.023$ ). No direct effects of nutrient supply were observed on biomass growth, wood density, or wood structure, except for a notable decrease in specific leaf area. These results suggest that, although fewer and larger conduits may render the xylem more vulnerable to embolism formation under drought conditions, the high growth rate in sessile oak saplings under elevated CO<sub>2</sub> is supported by an efficient vascular system and may increase biomass production in this tree species. Nevertheless, the decreased mechanical strength, indicated by low density and xylem vulnerability to drought, may lead to earlier mortality, offsetting the positive effects of elevated CO<sub>2</sub> levels in the future.

had no role in study design, data collection and analysis, decision to publish, or preparation of the manuscript.

**Competing interests:** The authors have declared that no competing interests exist.

## 1. Introduction

Global atmospheric CO<sub>2</sub> concentration has increased by more than 45% since the industrial revolution began, reaching above 410 ppm in 2020 [1]. By and large, this substantial increase has been caused by CO<sub>2</sub> released from anthropogenic emissions, such as the burning of fossil fuels, deforestation, and other land-use changes. Currently, the average rate of increase in atmospheric CO<sub>2</sub> concentration is 2 ppm per year, whereby the global atmospheric CO<sub>2</sub> level is likely to increase to 550–1000 ppm by the end of the century [2], depending on the success of our efforts to reduce CO<sub>2</sub> emissions [3]. Further, elevated CO<sub>2</sub> concentrations (hereafter, eCO<sub>2</sub>) are the main cause of global warming and are predicted to cause an increase in air temperature from 2 to 5 °C by the end of the 21<sup>st</sup> century [3]. Through photosynthesis, forests sequester approximately 26% of anthropogenic carbon emissions each year [4], thus playing an important role in preventing global warming. Additionally, an increase in anthropogenic nitrogen deposition enhances soil nitrogen availability, which may reportedly hinder the CO<sub>2</sub>-sequestering ability of plants [5, 6].

Numerous studies have demonstrated the effects of eCO<sub>2</sub> levels on plant growth and function over the last few decades [7–12], wherein increased atmospheric CO<sub>2</sub> levels were shown to improve tree growth through a process known as the “fertilisation effect”. Photosynthesis is directly influenced by variations in CO<sub>2</sub> concentrations and is one of the most studied physiological processes. Previous studies have shown that at the leaf level, eCO<sub>2</sub> concentrations increase photosynthesis rates while reducing stomatal conductance, thereby enhancing water use efficiency (WUE) [13–16]. The carbohydrates produced in the process serve as the building blocks for plant biomass production and many other processes in which carbon is metabolised [17]. Therefore, the enhancement of photosynthesis and the resulting carbohydrate surplus promoted by eCO<sub>2</sub> levels lead to a consistent increase in biomass growth. However, these effects have been mostly observed in young saplings [10, 14, 18], whereas mature trees usually do not show a positive growth response to eCO<sub>2</sub> levels [19]. In addition, growth stimulation by eCO<sub>2</sub> may be limited by the progressive scarcity of soil nutrients, particularly nitrogen [20–24]. Indeed, the effects of N deficiency on eCO<sub>2</sub>-induced growth stimulation are evident in plants growing on severely nutrient-deficient substrates [25]. Thus, any generalisation of plant responses to nutrient unavailability under eCO<sub>2</sub> levels is difficult to make [13].

Although previous studies have investigated the effects of eCO<sub>2</sub> levels on plant physiological and growth responses, few studies have addressed the changes in wood structure resulting from elevated CO<sub>2</sub> concentrations [26]. Furthermore, the changes in the physiology and growth of a plant not only alter the internal water balance [27] but also affect the structure and functioning of tracheids and vessel elements in the secondary xylem [28, 29] as well as xylem hydraulic conductance [30]. Nonetheless, the effects of eCO<sub>2</sub> levels on xylem elements vary among species. For instance, the tracheid lumen area in coniferous species such as *Larix sibirica* Ledeb. [31] and *Pinus sylvestris* L. [29] increased under eCO<sub>2</sub> levels. In contrast, diffuse-porous tree species were less responsive to eCO<sub>2</sub> levels and no effect was observed on the vessel area in *Populus tremuloides* Michx. [32], *Betula pendula* Roth. [33], or *Fagus sylvatica* L. [34]. Moreover, the lesser-investigated ring-porous tree species showed inconsistent results under eCO<sub>2</sub> levels, for example, increased vessel area in *Quercus robur* L. [35] but no changes in *Quercus mongolica* Fisch. Ex Ledeb. [28, 36]. Nevertheless, Watanabe et al. [28] also observed wider vessels and higher hydraulic conductance in *Q. mongolica* trees grown in N-rich soil regardless of CO<sub>2</sub> concentration.

The lumen area of xylem conduits is an important factor that influences not only the water flux capacity of xylem [37] but also wood density. Wood density is a key determinant of plant ecological strategies [38], including both hydraulic and mechanical strategies, as denser wood

is more resistant to cavitation and is stiffer and less susceptible to wind damage [39]. Increased plant growth rate is another wood density-related factor associated with lower wood density [40–42] that renders fast-growing trees more susceptible to high winds [43]. Information about the effect of eCO<sub>2</sub> on wood density is rather scarce in the literature. Conifers are known to exhibit higher wood density under eCO<sub>2</sub>, owing to their characteristically higher proportion of latewood. In contrast, angiosperms show no changes in wood density under eCO<sub>2</sub> levels [26]; however, they have been much less studied.

Therefore, with the simultaneous increase in CO<sub>2</sub> levels and nitrogen deposition in the coming decades, forest ecosystems will face many challenges that will force plants to adapt to warmer temperatures, higher evaporative demand, and increased frequency and severity of drought events [44]. Nonetheless, as difficult as it may seem to predict how forests will respond to these changes, the range of tree species in Central Europe will likely be substantially altered from the presently dominant conifers, to angiosperms, particularly thermophilous oak species [45, 46].

Sessile oak (*Quercus petraea* (Matt.) Liebl.), a broad-leaved, ring-porous tree species, is widespread in the temperate zone and is one of the most ecologically and economically important hardwood tree species in Central Europe [47, 48]. Owing to the morphological (deep rooting, leaf curling, and leaf loss) and physiological (osmotic adjustment and stomatal control to reduce transpiration water loss) mechanisms to overcome drought stress [49, 50], sessile oaks are considered well adapted for future climate scenarios [51, 52].

Therefore, the objective of this study was to investigate the effects of (i) eCO<sub>2</sub> concentration and (ii) nutrient supply on biomass growth, wood density, and wood structure of the conductive tissue in sessile oak saplings. Our main hypothesis was that the growth of sessile oak saplings will be stimulated by the fertilisation effect of eCO<sub>2</sub>. Previous studies have reported that higher growth rates in sessile oak in Western and Central Europe are associated with lower wood density [41, 42, 53]; accordingly, we tested the hypothesis that eCO<sub>2</sub> concentration is the cause for the observed morphological difference. Furthermore, it was expected that the higher growth rates would be followed by altered wood anatomy, which in turn would be reflected in a larger more efficient conductive system. Finally, we also hypothesised that the magnitude of the CO<sub>2</sub> fertilisation effect is regulated by nutrient supply.

## 2. Materials and methods

### 2.1. Study area

The experiment was conducted in two neighbouring glass domes (area: 10 × 10 m<sup>2</sup>; central height: 7 m) in the Bílý Kříž experimental ecological station situated in the Moravian-Silesian Beskydy mountains (49° 30' 77" N, 18° 32' 28" E; Elevation: 908 m asl). The mean air temperature and the mean precipitation during the period 1998–2014 were 6.8 °C and 1,260 mm, respectively. The soil type is ferric podzol, overlying the Mesozoic Godula sandstone (flysch-type), which is moderately rich and has a high humus content (5%–7%).

Under the scenario that has most closely tracked human historical emission trajectories, the atmospheric CO<sub>2</sub> concentrations will reach approximately 550 to 700 ppm by the middle-to-late 21st century [2, 3]. Previous studies on the effect of elevated CO<sub>2</sub> on different tree species were conducted mostly based on these concentrations [16, 54, 55], whereas more pessimistic predictions of 900–1000 ppm, which are expected by the end of 21 century, have been rarely used [13, 18]. In our study, ambient CO<sub>2</sub> (hereafter aCO<sub>2</sub>) and eCO<sub>2</sub> treatment concentrations in the open-top glass domes were 400 and 700 ppm, respectively, and CO<sub>2</sub> was continuously supplied from April to November, from 2017 to 2019. The design and installation of the glass domes was as described previously [56]. The microclimatic conditions inside the two domes

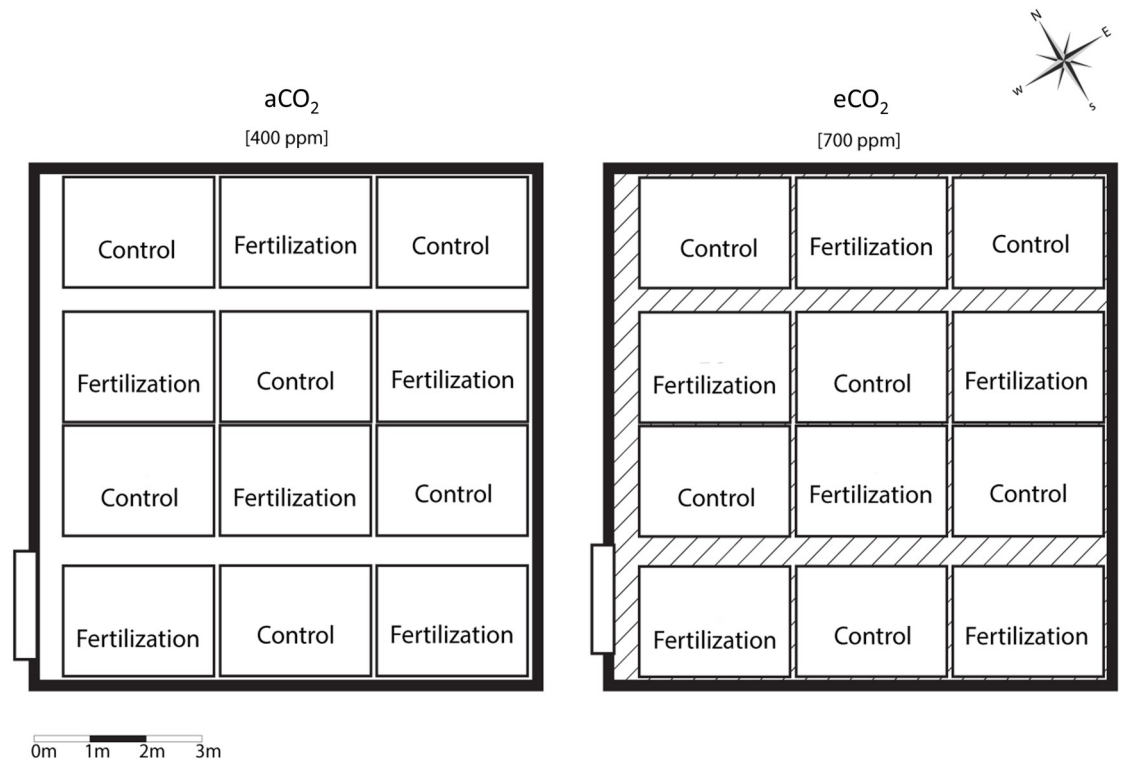


**Fig 1. Experimental design scheme.** aCO<sub>2</sub>—ambient CO<sub>2</sub> concentration, eCO<sub>2</sub>—elevated CO<sub>2</sub> concentration, Control—plots without nutrient supply, Fertilization—plots with nutrient supply.

<https://doi.org/10.1371/journal.pone.0259054.g001>

were maintained at similar levels, as shown by the non-significant differences in temperature ( $p = 0.953$ ) and relative air humidity ( $p = 0.485$ ). The soil inside the glass domes was natural and not mechanically altered, representing the same soil type as at the study site.

A total of 144 two-year-old sessile oak saplings were planted in each glass dome in 2017, following a specific fertilisation experimental design (Fig 1). Each glass dome was split into twelve blocks: no fertiliser was added to six blocks (control), while the other six blocks were annually supplied with calcium nitrate (AGRO, Czech Republic) containing 15% nitrogen, at a rate of  $5 \text{ g m}^{-2} \text{ year}^{-1}$  in mid-April during the study period (2018–2019).

## 2.2. Sampling and biometrical analyses

At the end of the growth season of 2019, we sampled all (72 per treatment) sessile oak saplings to compare their biometric characteristics. Before harvesting, plant height (H, cm) and stem diameter at a height of 5 cm above the ground ( $D_{0.05\text{m}}$ , mm) were recorded, and the cross-sectional area (CSA,  $\text{cm}^2$ ) was calculated using  $D_{0.05\text{m}}$ . Then, ten fresh leaves were randomly selected from the upper, middle, and bottom parts of the crown of each harvested oak sapling, scanned, and oven-dried at  $70^\circ\text{C}$  to measure their dry biomass using a precision scale (Radwag PS 6000.R1; precision: 0.01 g). Then, the specific leaf area (SLA;  $\text{cm}^2 \text{ g}^{-1}$ ) was calculated according to procedure described by Pietras et al. [42].

Subsequently, the above- and belowground biomass fractions of all samples were subdivided into leaves, branches, stems, and roots, which were further subdivided into coarse ( $> 2$  mm) and fine roots ( $\leq 2$  mm), based on root diameter. After measuring their fresh weight, the

fractions were oven-dried at 70 (leaves) and 105 °C (woody biomass) to constant weight [57], and their dry biomass ( $\text{g plant}^{-1}$ ) were measured. Then, SLA and leaf biomass were used to calculate the leaf area ( $\text{LA, m}^2 \text{ plant}^{-1}$ ) of each plant.

### 2.3. Wood density

To determine the density of oven-dried wood, 5–8 cm long wood segments from a height of 10 cm above the ground were collected from all saplings and oven-dried (as described above). Their dry biomass and volume were measured using a digital scale (see above) and the water displacement method based on the Archimedes' principle; briefly, a container filled with water was placed on the digital scale calibrated to the nearest 0.01 g and re-zeroed. The pith of each oven-dried wood segment was connected to a needle, and the segment was immersed into the water, ensuring that it did not touch the sides or bottom of the container. The weight of the water displaced was equal to the volume of the oven-dried segment, as 1 g of displaced water was equivalent to  $1 \text{ cm}^3$ . Subsequently, the wood density ( $\text{WD, g cm}^{-3}$ ) of the oven-dried sample was calculated as the dry biomass of the wood sample divided by its volume [29].

### 2.4. Anatomical measurements

Immediately after harvesting, 1.8 mm thick microcores were collected from the base of the stems of 18 saplings per treatment using a Trephor increment borer [58]. Following the methodology of Fajstavr [59], the samples were dehydrated in successive baths of ethanol and embedded in paraffin. Then, 8–12  $\mu\text{m}$  thick transverse wood sections were cut using a rotary microtome, stained in safranin and astra blue solutions, and mounted in Euparal. The cross-sections were then photographed using a digital video camera (Zeiss Axiocam 305 colour) attached to a light microscope (Zeiss Axio scope A1) at  $100\times$  magnification.

Two to three sectors of the outermost ring, formed in 2019 (third year of  $\text{CO}_2$ -enrichment experiment), from each cross-section were used to measure the width of the growth ring (RW) and the vessel lumen area (VLA) using ImageJ version 1.52a [60]. Cells with a lumen area  $\leq 200 \mu\text{m}^2$  were excluded to distinguish xylem vessels from other cell types [61]. Then, average VLA, vessel density (VD;  $\text{n mm}^{-2}$ ), total vessel lumen area (TVA;  $\mu\text{m}^2$ ), and the proportion of TVA per analysed sector (PTVA; %) were calculated as described by Lotfiomran et al. [34]. The lumen diameter of each circular vessel was derived from VLA and used to calculate their hydraulically weighed diameter ( $D_{\text{hp}}, \mu\text{m}$ ) according to the equation:

$D_{\text{hp}} = \left( \frac{\sum D^4}{N} \right)^{\frac{1}{4}}$ , where  $D$  is the diameter of the vessel and  $N$  is the number of vessels [37]. The

potential specific hydraulic conductivity of vessels ( $K_S; \text{kg m}^{-1} \text{ s}^{-1} \text{ MPa}^{-1}$ ) was calculated using the Hagen–Poiseuille equation [62]:  $K_S = \left( \frac{\pi \rho}{128 \eta} \right) D_{\text{hp}}^4 \text{VD}$ , where  $\eta$  is the viscosity of water ( $1,002 \times 10^{-9} \text{ MPa s}$ ),  $\rho$  is the density of water ( $998.21 \text{ kg m}^{-3}$ ),  $D_{\text{hp}}$  is the hydraulically weighed diameter of vessels, and  $\text{VD}$  is the mean vessel density. The potential hydraulic conductivity of a growth ring ( $K_{\text{ring}}; \text{kg m s}^{-1} \text{ MPa}^{-1}$ ) was estimated using the following equation by Noyer et al. [63]:  $K_{\text{ring}} = K_S \times \text{BAI}_{2019}$ , where the basal area increment of 2019 ( $\text{BAI}_{2019}; \text{cm}^2$ ) was calculated using the equation  $\text{BAI}_{2019} = \pi (R^2_{2019} - R^2_{2018})$ , where  $R$  is the radius of the tree in two subsequent years, 2018 and 2019 [64]. Subsequently, the xylem vulnerability index [65] was calculated by dividing the vessel diameter ( $D$ ) by  $\text{VD}$  to obtain a rough estimation of the xeromorphic or mesomorphic character of the stem xylem.

According to the Hagen–Poiseuille law, large earlywood vessels in ring-porous oak species play a dominant role in axial water flow, wherein a few large earlywood vessels can transport an equal amount of sap as that transported by many small latewood vessels [37, 62]. However,

the rationale of using all the vessels in the study was that the sampled wood sections had a semi-ring-porous to diffuse-porous structure instead of the ring-porous wood structure. In addition, the role of smaller vessels in ring-porous species is reportedly underestimated [66], considering their importance in tree survival when large vessels lose their transport capacity owing to drought-induced [67] or freeze-/thaw-induced embolism [68].

## 2.5. Statistical analyses

To assess the impact of CO<sub>2</sub> concentration and fertilisation on sessile oak saplings, a split-plot experimental design was applied. After examining the normality assumption and variance homogeneity of the data, two-way analysis of variance (ANOVA) was used to evaluate the effects of CO<sub>2</sub>, nutrient supply, and their interactions on each measured biometrical and wood anatomical parameter. Additionally, Duncan's method was used for the post-hoc comparisons of the treatment pairs. Non-normal data were transformed using a square root transformation and normality was then confirmed using the Kolmogorov–Smirnov test before performing the ANOVA.

Statistical analyses were performed using Statistica 13.0 (TIBCO Software Inc., Palo Alto, CA, USA), and statistical significance for all analyses was set at  $p \leq 0.05$ . Boxplots were created using the software SigmaPlot<sup>®</sup> 11.0 (Systat Software Inc., San Jose, CA, USA). Generalised additive models (GAMs) were fitted to each individual tree image using the mgcv package of R software [69], and average values were then calculated per treatment to evaluate the vessel-area size changes within the tree rings.

## 3. Results

### 3.1. Effects of eCO<sub>2</sub> and nutrient supply on biometrical characteristics

All aboveground morphological parameters measured were significantly affected by eCO<sub>2</sub> treatment, whereas nutrient supply did not significantly affect them, except for SLA ( $p = 0.021$ ) (Table 1). Furthermore, there was no significant effect of CO<sub>2</sub> concentration–nutrient supply interactions on the aboveground biomass (Table 1). We observed a significant increase in all the biometrical parameters (H,  $D_{0.05m}$ , and  $CSA_{0.05m}$ ) and all the aboveground biomass (i.e. leaves, branches, and stems) fractions (Fig 2, Table 1) under eCO<sub>2</sub> treatment. Moreover, LA of the saplings was increased by 27%, and SLA was decreased by approximately 5.4% under eCO<sub>2</sub> than under aCO<sub>2</sub> (Table 1).

Additionally, eCO<sub>2</sub> had a positive effect on total sapling biomass, with an increase of 49% (Table 1). In turn, nutrient supply had a non-significant positive effect (an increase of 12%) on total sapling biomass under aCO<sub>2</sub> treatment, whereas a non-significant negative effect (a decrease of 3%) was observed under eCO<sub>2</sub> treatment (Figs 2 and 3, S1 Table).

Furthermore, eCO<sub>2</sub> treatment had a positive effect on total belowground biomass, i.e. an increase of 47% in fine and coarse roots (Table 1). However, nutrient supply had a negative effect on both fine and coarse roots (Fig 3). The saplings growing under eCO<sub>2</sub> treatment had significantly higher amounts of fine roots (45%) than those growing under aCO<sub>2</sub> treatment.

### 3.2. Effects of eCO<sub>2</sub> and nutrient supply on wood structure

All wood anatomical parameters showed significant differences under eCO<sub>2</sub> treatment, except for TVA, PTVA, and  $K_s$ , whereas neither nutrient supply nor the interaction between CO<sub>2</sub> concentration and nutrient supply showed any influence on wood structure, except for BAI (Table 2). Larger vessels were observed in the earlywood and transition zones under eCO<sub>2</sub> treatment (tree-ring position <50%), while latewood zone vessels tended to display similar lumen area regardless of the CO<sub>2</sub> treatments (Fig 4).



**Table 1. Two-way analysis of variance (ANOVA) of the influence of CO<sub>2</sub>, nutrient supply and their interactions on sessile oak saplings aboveground and below-ground biometrical characteristics.**

	CO <sub>2</sub>		Nutrition		CO <sub>2</sub> × Nutrition	
	F	p	F	P	F	p
Height (cm)	4.15	<b>0.043</b> ↑	0.438	0.509	0.001	0.975
D <sub>0.05m</sub> (mm)	10.99	< <b>0.001</b> ↑	0.28	0.596	1.54	0.215
CSA <sub>0.05m</sub> (mm)	13.92	< <b>0.001</b> ↑	0.16	0.686	1.22	0.270
Leaf biomass (g)	6.22	<b>0.014</b> ↑	0.16	0.691	0.03	0.862
Branch biomass (g)	4.67	<b>0.033</b> ↑	0.03	0.857	0.02	0.893
Stem biomass (g)	7.77	<b>0.006</b> ↑	0.77	0.381	0.18	0.673
Total aboveground biomass (g)	7.36	<b>0.007</b> ↑	0.45	0.501	0.06	0.809
Fine root (≤2 mm) biomass (g)	25.03	< <b>0.001</b> ↑	0.13	0.716	0.02	0.884
Coarse root (>2mm) biomass (g)	12.91	< <b>0.001</b> ↑	1.67	0.198	0.77	0.382
Total belowground biomass (g)	14.65	< <b>0.001</b> ↑	1.49	0.223	3.19	0.435
Total plant biomass (g)	11.58	< <b>0.001</b> ↑	0.07	0.985	0.53	0.467
WD (g/cm <sup>3</sup> )	8.70	<b>0.003</b> ↓	2.70	0.102	0.00	0.961
LA (m <sup>2</sup> /plant)	6.65	<b>0.011</b> ↑	0.02	0.889	0.85	0.356
SLA (cm <sup>2</sup> g <sup>-1</sup> )	14.37	< <b>0.001</b> ↓	5.43	<b>0.021</b> ↓	0.75	0.390

D<sub>0.05m</sub>—diameter at 5 cm above ground; CSA<sub>0.05m</sub>—cross-sectional area at 5 cm above ground; WD—wood density; LA—leaf area; SLA—Specific leaf area;

↑—increase with eCO<sub>2</sub>;

↓—decrease with eCO<sub>2</sub>.

Statistically significant effects and interactions are indicated in bold ( $p \leq 0.05$ ).

<https://doi.org/10.1371/journal.pone.0259054.t001>

The VLA was significantly increased at eCO<sub>2</sub>, whereas VD was significantly lower (Fig 5, Table 2), with the highest VLA and lowest VD recorded in the saplings under eCO<sub>2</sub> treatment without nutrient supply (Fig 5, S2 Table). In contrast, TVA and PTVA showed no significant differences under eCO<sub>2</sub> as compared with aCO<sub>2</sub> (Table 2, S2 Table), and RW exhibited the largest increase under the nutrient supply plus eCO<sub>2</sub> combination treatment (Fig 5, S2 Table).

The values of all the traits associated with hydraulic conductivity increased under eCO<sub>2</sub> (Table 2), and the highest statistically significant values of D<sub>hp</sub> were observed in saplings under eCO<sub>2</sub> without nutrient supply (Fig 5, S2 Table). The K<sub>s</sub> values were not significantly different between any of the treatments (S2 Table), whereas K<sub>ring</sub> values were significantly higher in saplings grown at eCO<sub>2</sub> than in the saplings grown at aCO<sub>2</sub>, regardless of nutrient supply (Fig 5, S2 Table). Furthermore, the vulnerability index was significantly higher in the former case (Table 2), with the highest value observed in unfertilised saplings (Fig 5, S2 Table).

Overall, the saplings grown under eCO<sub>2</sub> concentration treatment had significantly lower densities (approximately 1.7%); however, nutrient supply or the CO<sub>2</sub>-concentration—nutrient -supply interaction had no effect (Table 1). Saplings with nutrient supplementation had lower wood densities than the saplings grown without nutrient supply under the two different CO<sub>2</sub> concentrations tested here; furthermore, the saplings grown with nutrient supply under eCO<sub>2</sub> exhibited significantly lower wood densities than those in any other treatment (Fig 6, S1 Table).

## 4. Discussion

### 4.1. Effects of eCO<sub>2</sub> on biometrical characteristics of sessile oak saplings

Our study revealed a high growth benefit for sessile oak saplings grown in the eCO<sub>2</sub> environment. After three years of exposure to eCO<sub>2</sub> concentration treatment, the saplings grew taller

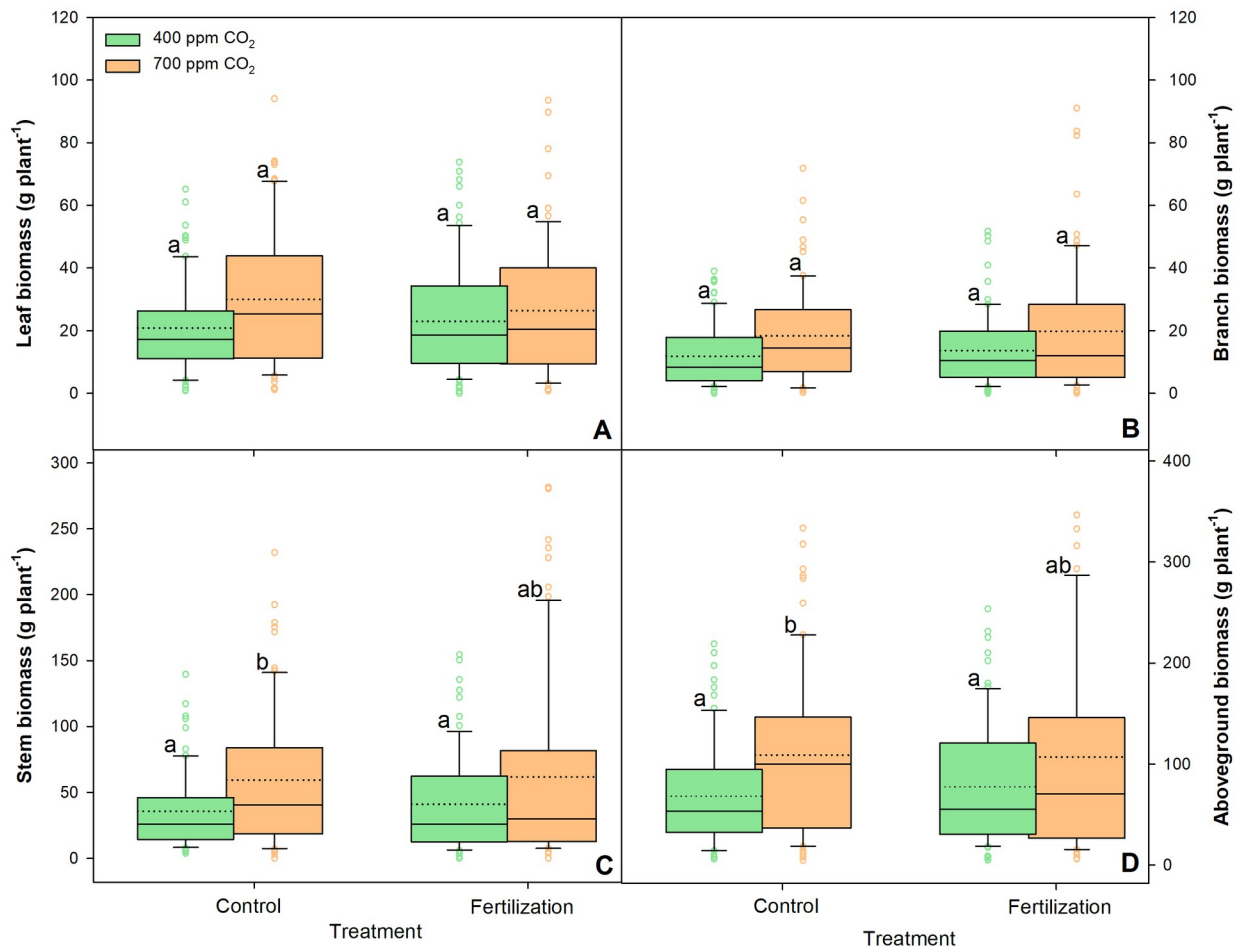


**Fig 2. Changes in leaf biomass (A), branch biomass (B), stem biomass (C), and above-ground biomass (D) of sessile oak saplings ( $n = 72$ ) treated under ambient (400 ppm  $\text{CO}_2$ ) and elevated (700 ppm  $\text{CO}_2$ ) and different nutrient supplies.** The data are expressed as medians (solid lines) and means (dotted lines) of measurements. The box boundaries mark the 25<sup>th</sup> and 75<sup>th</sup> percentiles and whiskers the 10<sup>th</sup> and 90<sup>th</sup> percentiles. Circles marks outliers. Different letters indicate significant differences ( $p \leq 0.05$ ) estimated on the basis of Duncan's ANOVA post-hoc test.

<https://doi.org/10.1371/journal.pone.0259054.g002>

and wider stems and accumulated 49% more dry biomass (both above- and belowground) than the saplings grown under a $\text{CO}_2$  concentration treatment (Figs 2 and 3, Table 1). Previous studies have shown growth stimulation in young saplings of many different tree species in response to e $\text{CO}_2$  [10, 70]. In sessile oak saplings grown under e $\text{CO}_2$ , Ofori-Amanfo et al. [15] revealed an increase in the light-saturated  $\text{CO}_2$  assimilation rate, a decrease in stomatal conductance, and consequently improved WUE. Evidently, e $\text{CO}_2$  concentrations directly influence plant growth by increasing photosynthesis and decreasing stomatal conductance, resulting in a subsequent increase in WUE and carbohydrate availability for growth, eventually leading to greater biomass production [12]. Consistent with our results, Saxe et al. [71] reported that e $\text{CO}_2$  significantly increased plant size and aboveground biomass, with angiosperms responding less (average increase of 49%) than conifers, which showed an average biomass increase of 130% (Figs 2 and 3, Table 1 and S1 Table).

Increased plant productivity is directly related to greater LA, which is crucial for radiation interception, photosynthetic assimilation, and, ultimately, plant growth and performance.



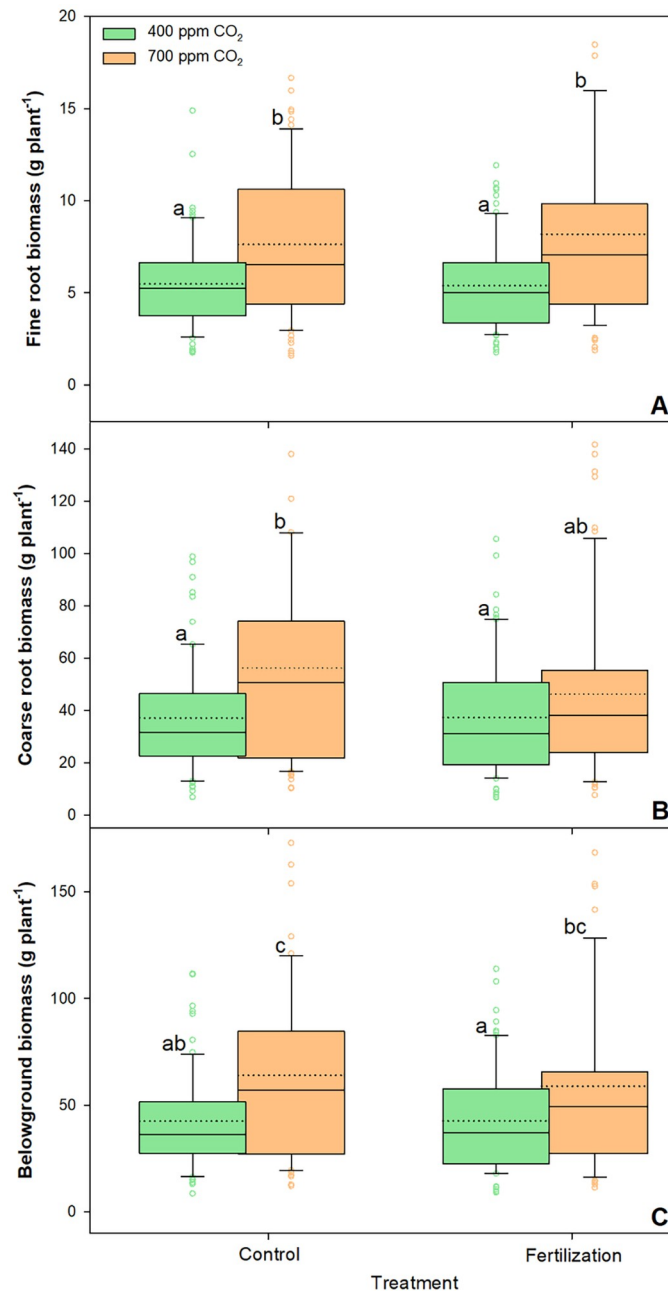


**Fig 3. Changes in fine roots biomass (A), coarse roots biomass (B), and belowground biomass (C) of sessile oak saplings (n = 72) treated under ambient (400 ppm CO<sub>2</sub>) and elevated (700 ppm CO<sub>2</sub>) and different nutrient supplies.** The data are expressed as medians (solid lines) and means (dotted lines) of measurements. The box boundaries mark the 25th and 75th percentiles and whiskers the 10th and 90th percentiles. Circles mark outliers. Different letters indicate significant differences ( $p \leq 0.05$ ) estimated on the basis of Duncan's ANOVA post-hoc test.

<https://doi.org/10.1371/journal.pone.0259054.g003>

Previous studies have reported larger LA and leaf biomass and reduced SLA in plants growing under eCO<sub>2</sub> [11]. This study also showed that LA increased by 27% and SLA decreased by 5.4% in saplings grown under eCO<sub>2</sub> treatment (Table 1 and S1 Table). Evidence suggest that eCO<sub>2</sub> affects plant cell proliferation by enhancing cell division and cell enlargement [30], although, according to Pritchard et al. [11], increased leaf growth under eCO<sub>2</sub> conditions is

**Table 2. Two-way analysis of variance (ANOVA) of the influence of CO<sub>2</sub>, nutrient supply, and their interactions on sessile oak saplings anatomical characteristics.**

	CO <sub>2</sub>		Nutrition		CO <sub>2</sub> × Nutrition	
	F	p	F	p	F	p
Vessel diameter (μm)	8.06	<b>0.006</b> ↑	0.34	0.560	0.42	0.519
VLA (μm <sup>2</sup> )	9.32	<b>0.003</b> ↑	0.69	0.410	0.74	0.394
TVA (μm <sup>2</sup> )	0.56	0.455	0.34	0.560	1.49	0.226
PTVA (%)	0.56	0.459	0.58	0.450	0.25	0.621
D <sub>hp</sub> (μm)	8.69	<b>0.004</b> ↑	0.49	0.484	2.19	0.143
RW (μm)	8.31	<b>0.005</b> ↑	0.50	0.483	0.02	0.891
BAI (mm <sup>2</sup> )	11.61	<b>0.001</b> ↑	0.53	0.471	4.20	<b>0.044</b>
VD (N <sub>o</sub> mm <sup>-2</sup> )	5.43	<b>0.023</b> ↓	0.59	0.443	0.62	0.434
K <sub>s</sub> (kg m <sup>-1</sup> s <sup>-1</sup> MPa <sup>-1</sup> )	0.46	0.499	0.13	0.722	0.40	0.531
K <sub>ring</sub> (kg m s <sup>-1</sup> MPa <sup>-1</sup> )	7.88	<b>0.007</b> ↑	0.55	0.461	2.44	0.123
Vulnerability index	14.57	<b>0.001</b> ↑	1.73	0.192	1.27	0.263

VLA—Vessel lumen area; TVA—total lumen vessel area; PTVA—the proportion of the total vessel lumen area per analyzed sector; D<sub>hp</sub>—hydraulic weighted diameter; RW—ring width; BAI—Basal area increment; VD—Vessel density; K<sub>s</sub>—potential specific hydraulic conductivity; K<sub>ring</sub>—potential hydraulic conductivity for a growth ring; Vulnerability index was calculated after Carlquist [65].

↑—increase with eCO<sub>2</sub>;

↓—decrease with eCO<sub>2</sub>.

Statistically significant effects and interactions are indicated in bold ( $p \leq 0.05$ ).

<https://doi.org/10.1371/journal.pone.0259054.t002>

the result of cell proliferation stimulated by cell enlargement rather than cell division. Cell enlargement under eCO<sub>2</sub> levels is achieved by the decreasing osmotic potential in the cell driven by excess carbohydrates in the sap, which in turn promotes further water intake by the cell, thereby increasing turgor-driven cell wall enlargement [72]. Nevertheless, under eCO<sub>2</sub> conditions, the properties of the cell wall might be altered, and the cells may stretch to a greater extent than cells developing under lower CO<sub>2</sub> concentrations [73].

However, the tree response to eCO<sub>2</sub> is rather complex and we need to take into account complex interactions among CO<sub>2</sub> concentrations, photosynthesis and other environmental factors, as well as even more complex relationships among carbon assimilation, plant respiration and growth [9, 10, 16]. For example, mature trees do not show greater biomass production under eCO<sub>2</sub> despite the stimulated photosynthesis [19] suggesting that C availability itself is not necessarily the most limiting factor for tree growth [74, 75]. Instead, it was suggested that growth is limited by environment, and in particular water stress limits the ability of cambium to convert the carbon into growth [76]. In fact, many studies on different plant species have shown that during heat and water stress, C demand for growth always declines before photosynthesis (carbon supply) is affected [74, 75]. However the surplus in carbon is usually allocated in different sink other than growth (biomass), such as respiration [9, 19]. Thus, climate changes are widely expected to increase more extreme weather events, in particular heat and drought stress [44, 45], which will certainly mitigate the potential of eCO<sub>2</sub> to stimulate tree growth in many regions [9].

#### 4.2. Effects of eCO<sub>2</sub> on wood structure of sessile oak saplings

Yazaki et al. [31] reported that both enhanced cell division and cell enlargement were responsible for increased wood formation under eCO<sub>2</sub> conditions. In this study, sessile oak saplings grown under eCO<sub>2</sub> treatment exhibited significantly increased RW, BAI, VLA, and,

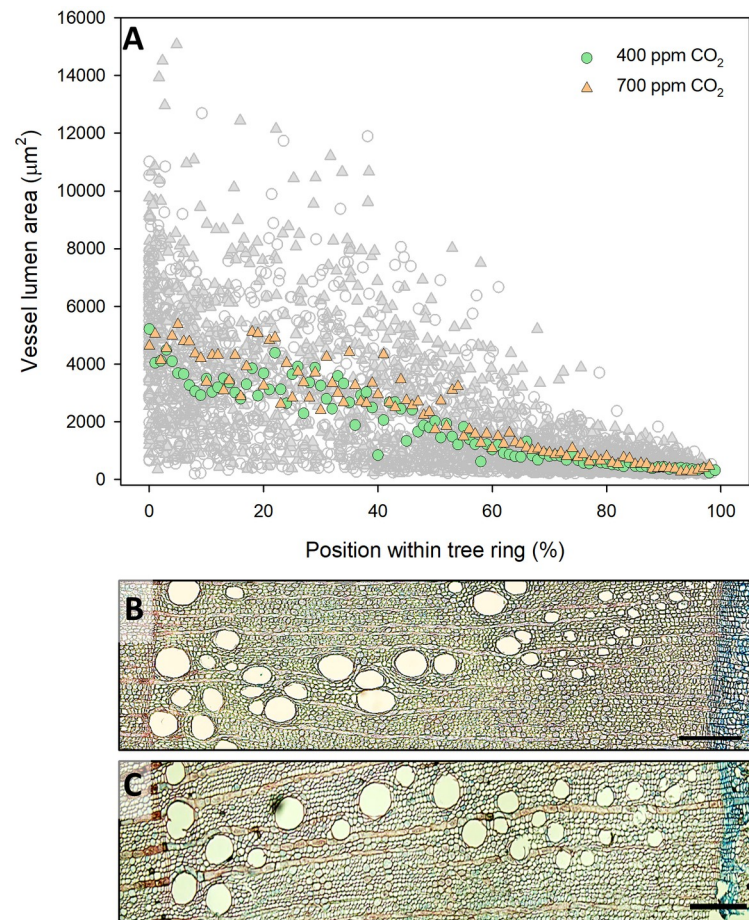


**Fig 4. Overview of tree ring in 2019.** (A) The relative position of vessel lumen areas within tree ring created in 2019 with applied GAMs denoted by orange (elevated CO<sub>2</sub>) and green characters (ambient CO<sub>2</sub>). Microscope images of a cross-section of the 2019 annual ring of a sessile oak saplings growing in (B) ambient CO<sub>2</sub> glass dome and (C) elevated CO<sub>2</sub> glass dome. Scale bars = 200 µm.

<https://doi.org/10.1371/journal.pone.0259054.g004>

consequently, xylem hydraulic conductance (Figs 4 and 5, Table 2 and S2 Table). Wood formation is affected by cambial activity, which in turn may be affected by eCO<sub>2</sub> concentrations. Consistently, Watanabe et al. [36] reported a high number of active cambium cells in two ring-porous species under eCO<sub>2</sub> conditions, implying that the rate of cell division might be affected under varying CO<sub>2</sub> concentrations [5]. Moreover, the systematic review by Yazaki et al. [26] reported that the diameter and number of angiosperm xylem conduits increased owing to the changes in the inner water balance induced by eCO<sub>2</sub>. This was confirmed in the ring-porous *Q. robur* saplings, where both size and density of the vessels increased under eCO<sub>2</sub>, resulting in a two-fold increase in TVA [35]. The results of our study are partly in agreement with the findings of the above study, because we observed an increased VLA and a significantly decreased VD in the saplings grown under eCO<sub>2</sub>, whereas TVA remained unchanged (Fig 5, Table 2).

Although information on the effects of eCO<sub>2</sub> conditions on WD is limited and the results of previous studies are inconsistent [5, 26, 29, 30], eCO<sub>2</sub> conditions reputedly affect the duration or extent of secondary cell wall deposition in addition to cell division and enlargement [5, 26, 77]. Domec et al. [30] reported that photosynthesis stimulation under eCO<sub>2</sub> yielded sufficient building material for both thicker cell walls and sustained cell wall enlargement, which

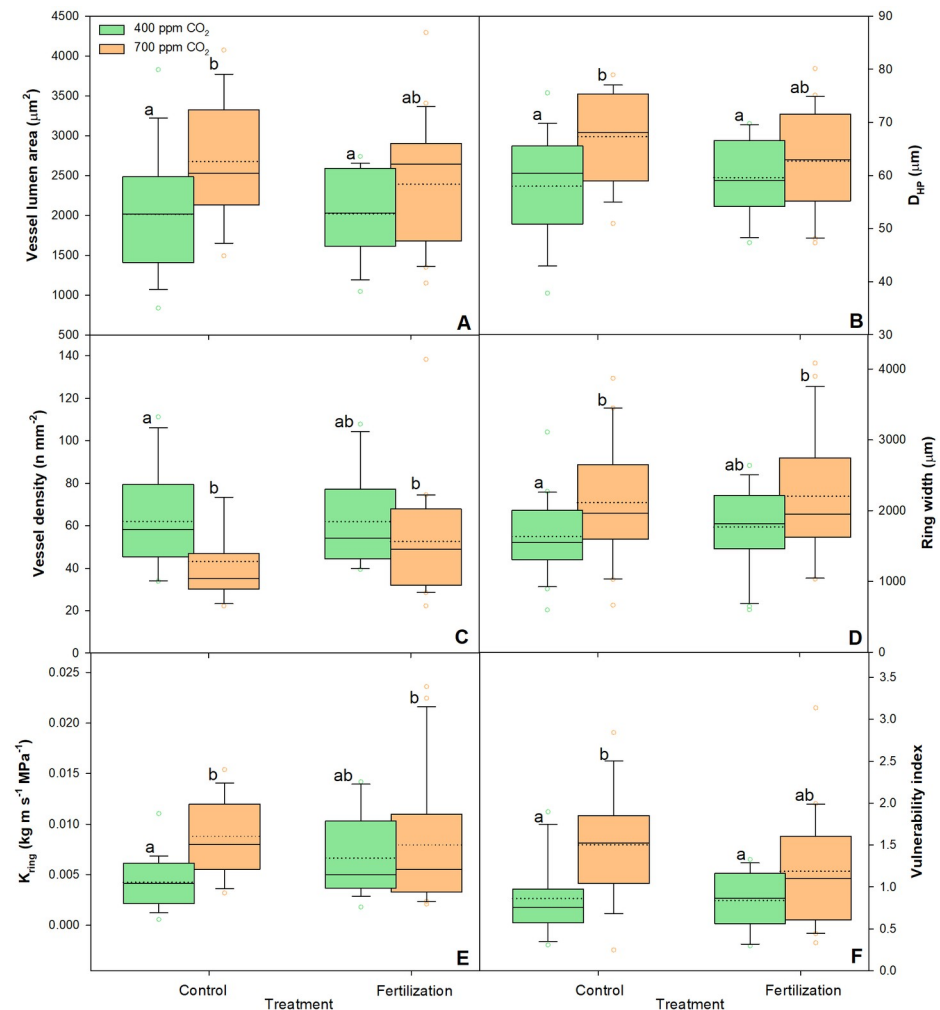


**Fig 5. Changes in vessel lumen area (A),  $D_{HP}$  (B), vessel density (C), Ring width (D),  $K_{ring}$  (E), and Vulnerability index (F) of sessile oak saplings ( $n = 18$ ) treated under ambient (400 ppm  $CO_2$ ) and elevated (700 ppm  $CO_2$ ) and different nutrient supplies.** The data are expressed as medians (solid lines) and means (dotted lines) of measurements. The box boundaries mark the 25<sup>th</sup> and 75<sup>th</sup> percentiles and whiskers the 10<sup>th</sup> and 90<sup>th</sup> percentiles. Circles mark outliers. Different letters indicate significant differences ( $p \leq 0.05$ ) estimated on the base of Duncan's ANOVA post-hoc test.

<https://doi.org/10.1371/journal.pone.0259054.g005>

simultaneously increased WD and xylem conductivity. However, these findings are partly in agreement with those of Yazaki et al. [31], who suggested a major effect of eCO<sub>2</sub> concentrations on cell division and enlargement rather than on cell wall deposition, resulting in a low WD in *L. sibirica* saplings growing under eCO<sub>2</sub> treatment. The findings of Yazaki et al. [31] are consistent with our study results, which revealed a significantly low WD in saplings growing under eCO<sub>2</sub> (Fig 6, Table 1).

The tree ring structure, defined by the number and dimensions of the constituent cells, is the primary determinant of WD. Angiosperm wood is a complex tissue that comprises vessels to conduct water, fibres to provide mechanical support, and parenchyma cells to store nutrients; furthermore, their relative proportions in the wood influences WD [39]. Vessels of ring-porous tree species have wider lumens than those in other wood cells. Moreover, vessel lumens have zero density and consequently negatively affect WD [78, 79]. However, we could not

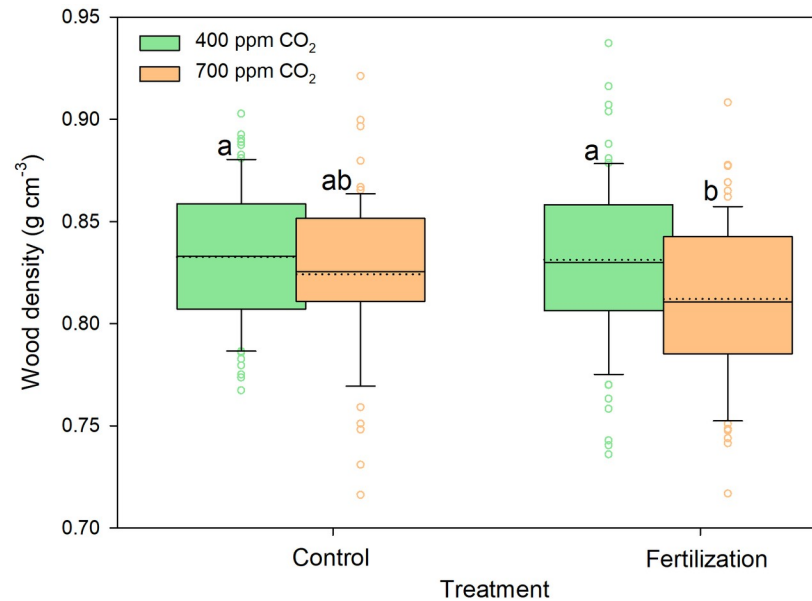


**Fig 6. Changes in over-dry wood density of sessile oak saplings ( $n = 72$ ) treated under ambient (400 ppm  $\text{CO}_2$ ) and elevated (700 ppm  $\text{CO}_2$ ) and different nutrient supplies.** The data are expressed as medians (solid lines) and means (dotted lines) of measurements. The box boundaries mark the 25<sup>th</sup> and 75<sup>th</sup> percentiles and whiskers the 10<sup>th</sup> and 90<sup>th</sup> percentiles. Circles mark outliers. Different letters indicate significant differences ( $p \leq 0.05$ ) estimated on the base of Duncan's ANOVA post-hoc test.

<https://doi.org/10.1371/journal.pone.0259054.g006>

verify this observation in this study, as no statistical differences in TVA or PTVA were observed between saplings grown under the a $\text{CO}_2$  and e $\text{CO}_2$  treatments (Table 2 and S2 Table). Therefore, other anatomical characteristics, such as fibres, living parenchyma [39], and cell wall thickness of each cell type [77] may be responsible for the low WD in the saplings grown in an e $\text{CO}_2$  environment. As this study was limited to wood anatomy of the conductive tissue in the last formed ring, we cannot draw any definite conclusions regarding this issue.

Moreover, studies by Bergès et al. [53] and Pretzsch et al. [41] reported long-term increased growth and reduced WD in sessile oak trees using dendrochronological and long-term inventory data, respectively, which are in agreement with our observations. Additionally, Pretzsch et al. [41] suggested that N supply via atmospheric deposition might be a major reason for a decrease in WD, rather than the increase in  $\text{CO}_2$  concentration, which contradicts our results (Table 1). Nevertheless, although we observed the highest WD decrease in the saplings grown with nutrient supplementation under the e $\text{CO}_2$  treatment (Fig 6), we unexpectedly did not find significant effects of the interaction between  $\text{CO}_2$  concentration and nutrient supply (Table 1).

### 4.3. Response of sessile oak saplings to nutrient supply

Neither nutrient supply nor its interaction with  $\text{CO}_2$  concentration exhibited any significant effect on the experimental saplings, except for SLA (Tables 1 and 2). Similar results were reported by Lotfiomran et al. [34], who found that the anatomical features in *F. sylvatica* saplings were more strongly affected by e $\text{CO}_2$  than by fertilisation. Similarly, although e $\text{CO}_2$  enhanced the growth of *Quercus alba* saplings on N-limited soils, tissue N concentrations were significantly reduced compared to those in saplings grown under a $\text{CO}_2$  treatment [80]. This implies that plants under e $\text{CO}_2$  concentration were highly efficient, with less investment in

their tissue [81], which was indirectly verified in our study via the reduced WD measured in the saplings grown under eCO<sub>2</sub> treatment (Table 1).

The increase in sapling growth observed in our study required sufficient nutrients to take advantage of the eCO<sub>2</sub> condition; that increased nutrient demand was met by the relatively fertile native soil where the saplings were planted. It has been demonstrated that eCO<sub>2</sub> conditions accelerate the effects of nutrient unavailability with time [21–23]. For instance, Rolo et al. [82] reported that the enhanced growth in *F. sylvatica* and *Picea abies* Karst. saplings induced by eCO<sub>2</sub> rendered the soil nutrient-deficient after six years. Therefore, we hypothesise that nutrient limitation in the glass dome supplied with eCO<sub>2</sub> treatment will develop gradually and eventually hinder the CO<sub>2</sub>-induced increase in plant biomass productivity [21].

#### 4.4. Possible implications on future forest management

Higher biomass production in sessile oak saplings under eCO<sub>2</sub> treatment was supported by an efficient xylem hydraulic system (Tables 1 and 2). However, the trade-off between hydraulic efficiency and safety (the ability of xylem to resist the formation and spread of embolisms) suggest that xylem comprising larger vessels may be less resistant to embolism during severe drought [83]. Similar to our findings, Levanic et al. [84] observed higher  $D_{hp}$ , BAI, and consequently  $K_{ring}$  in dead *Q. robur* trees than in the trees that survived a drought period, suggesting that the trees which died had been hydraulically maladjusted for dry conditions. This was also verified by the higher vulnerability index [65] observed in the saplings grown under eCO<sub>2</sub> in our study (Fig 5, Table 2). According to the principles of Carlquist's vulnerability index, saplings with wider and less abundant vessels express higher vulnerability indices and a higher mesic character, which are reflected in xylem conduits that are less resistant to embolism. However, enhanced WUE and larger absorptive area of the root system under eCO<sub>2</sub>, indicated by the increased biomass of both fine and coarse roots (Fig 3, Table 1), might compensate for xylem susceptibility and increase drought-resistance in sessile oak saplings [15]. Nevertheless, root capacity for water-uptake depends not only on root mass but also rooting depth as well as the area and activity of fine roots [11].

In this study, we found a significant effect of eCO<sub>2</sub> treatment on WD (Fig 6, Table 1), which is reportedly associated with many wood characteristics [39]. Low WD is well associated with reduced wood stiffness and strength [85], as has been observed in conifer and angiosperm saplings growing under eCO<sub>2</sub> conditions [29, 77], and higher susceptibility to wind and snow [43]. However, tree performances in response to mechanical constraints, such as wind or snow, are driven mainly by tree allometry, where the increase in stem diameter improves the fourth power resistance of stem to bending [86, 87] and proportionally to another mechanical stability trait [88]. Our results suggested that the mechanical performances are relayed by the improved growth rate under eCO<sub>2</sub> and that the decrease in WD reflects the adjustments of the hydraulic system and management of construction cost to the increasing stem volume. Nevertheless, storm-mediated forest damage has increased in recent decades [89]. As suggested by Pretzsch et al. [41], although changes in forest management are primarily responsible for these observations, low mechanical stability—as indicated by lower WD values—might also contribute to forest damage.

Our study focused on juvenile wood, and it is uncertain how mature trees will respond to future atmospheric conditions, though correlations between the qualities of juvenile and mature wood have been reported [90]. However, Pretzsch et al. [41] reported that unlike older trees with denser and more stable wood, young saplings growing under conditions leading to lower WD and less mechanical stability will be more affected by high winds [43]. Moreover, a



recent study on tree ring-growth in many species and environments found that faster tree ring-growth directly reduces tree lifespan [91].

Therefore, despite the increased biomass production at eCO<sub>2</sub> in this economically and ecologically important European tree species, the impacts of lower density on mechanical strength, and xylem becoming more vulnerable to drought, may lead to earlier mortality offsetting the positive effect of future eCO<sub>2</sub>.

## Supporting information

**S1 Table. Biometric characteristics of (*Quercus petraea* (Matt.) Liebl.) saplings under different CO<sub>2</sub> concentrations and nutrient supplies.** The data represent mean ( $\pm$  standard error of the mean). Different letters indicate significant differences ( $p \leq 0.05$ ) estimated on the basis of Duncan's ANOVA post-hoc test. D<sub>0.05m</sub>—diameter at 5 cm above ground; CSA<sub>0.05m</sub>—cross-sectional area at 5 cm above ground; LA—leaf area; SLA—Specific leaf area. (DOCX)

**S2 Table. Vessel anatomy characteristics of (*Quercus petraea* (Matt.) Liebl.) saplings under different CO<sub>2</sub> concentrations and nutrient supplies.** The data represent mean ( $\pm$  standard error of the mean). Different letters indicate significant differences ( $p \leq 0.05$ ) estimated on the basis of Duncan's ANOVA post-hoc test. TVA—Total vessel lumen area; PTVA—the proportion of the total vessel lumen area per analyzed sector; D<sub>hp</sub>—hydraulic diameter; VD—vessel density; TRW<sub>2019</sub>—Tree ring width; BAI<sub>2019</sub>—Basal area increment; K<sub>s</sub>—Potential specific hydraulic conductivity; K<sub>ring</sub>—potential hydraulic conductivity for a growth ring; VI—Vulnerability index calculated after Carlquist [65]. (DOCX)

## Acknowledgments

The authors are sincerely grateful to Martin Benz and Jiří Šlížek for their invaluable help during sampling campaigns. Further, the authors acknowledge SILVATECH from UMR 1434 SILVA, 1136 IAM, 1138 BEF, and 4370 EA LERMAB EEF research centre INRA Nancy-Lorraine for the development of ImageJ macro.

## Author Contributions

**Conceptualization:** Marko Stojanović, Jan Světlík, Jan Krejza.

**Data curation:** Marko Stojanović.

**Formal analysis:** Janko Arsić, Marko Stojanović, Estelle Noyer, Slobodan Milanović.

**Funding acquisition:** Petr Horáček.

**Investigation:** Janko Arsić, Marko Stojanović, Lucia Petrovičová, Jan Světlík, Jan Krejza.

**Methodology:** Janko Arsić, Marko Stojanović, Jan Světlík, Jan Krejza.

**Resources:** Petr Horáček, Jan Krejza.

**Supervision:** Jan Krejza.

**Validation:** Marko Stojanović.

**Visualization:** Marko Stojanović, Jan Krejza.

**Writing – original draft:** Janko Arsić, Marko Stojanović.

**Writing – review & editing:** Marko Stojanović, Lucia Petrovičová, Estelle Noyer, Slobodan Milanović, Jan Světlík, Petr Horáček, Jan Krejza.

## References

1. Dlugokencky E, Tans P. Trends in atmospheric carbon dioxide, National Oceanic & Atmospheric Administration, Earth System Research Laboratory (NOAA/ESRL). 2020 [cited 20 Apr 2021]. <http://www.esrl.noaa.gov/gmd/ccgg/trends/global.html>
2. van Vuuren DP, Edmonds J, Kainuma M, Riahi K, Thomson A, Hibbard K, et al. The representative concentration pathways: An overview. *Clim Change*. 2011; 109: 5–31. <https://doi.org/10.1007/s10584-011-0148-z>
3. Ciais P, Sabine C, Bala G, Bopp L, Brovkin V, Canadell J, et al. Carbon and Other Biogeochemical Cycles. In: Intergovernmental Panel on Climate Change, editor. *Climate Change 2013—The Physical Science Basis*. Cambridge: Cambridge University Press; 2013. pp. 465–570.
4. Pan Y, Birdsey RA, Fang J, Houghton R, Kauppi PE, Kurz WA, et al. A large and persistent carbon sink in the world's forests. *Science* (80-). 2011; 333: 988–993. <https://doi.org/10.1126/science.1201609> PMID: 21764754
5. Hättenschwiler S, Schweingruber FH, Körner C. Tree ring responses to elevated CO<sub>2</sub> and increased N deposition in *Picea abies*. *Plant, Cell Environ*. 1996. <https://doi.org/10.1111/j.1365-3040.1996.tb00015.x>
6. Churkina G, Brovkin V, Von Bloh W, Trusilova K, Jung M, Dentener F. Synergy of rising nitrogen depositions and atmospheric CO<sub>2</sub> on land carbon uptake moderately offsets global warming. *Global Biogeochem Cycles*. 2009; 23: 1–12. <https://doi.org/10.1029/2008GB003291>
7. Norby RJ, Wullschlegel SD, Gunderson CA, Johnson DW, Ceulemans R. Tree responses to rising CO<sub>2</sub> in field experiments: implications for the future forest. *Plant, Cell Environ*. 1999; 22: 683–714. <https://doi.org/10.1046/j.1365-3040.1999.00391.x>
8. Walker AP, De Kauwe MG, Bastos A, Belmecheri S, Georgiou K, Keeling R, et al. Integrating the evidence for a terrestrial carbon sink caused by increasing atmospheric CO<sub>2</sub>. *New Phytol*. 2020. <https://doi.org/10.1111/nph.16866> PMID: 32789857
9. Dusenge ME, Duarte AG, Way DA. Plant carbon metabolism and climate change: elevated CO<sub>2</sub> and temperature impacts on photosynthesis, photorespiration and respiration. *New Phytol*. 2019; 221: 32–49. <https://doi.org/10.1111/nph.15283> PMID: 29983005
10. Lauriks F, Salomón RL, Steppe K. Temporal variability in tree responses to elevated atmospheric CO<sub>2</sub>. *Plant Cell Environ*. 2020; 1–19.
11. Pritchard SG, Rogers HH, Prior SA, Peterson CM. Elevated CO<sub>2</sub> and plant structure: A review. *Glob Chang Biol*. 1999; 5: 807–837. <https://doi.org/10.1046/j.1365-2486.1999.00268.x>
12. Ceulemans R, Mousseau M. Tansley Review No. 71 Effects of elevated atmospheric CO<sub>2</sub> on woody plants. *New Phytol*. 1994; 127: 425–446. <https://doi.org/10.1111/j.1469-8137.1994.tb03961.x>
13. Lotfiomran N, Köhl M, Fromm J. Interaction effect between elevated CO<sub>2</sub> and fertilization on biomass, gas exchange and C/N ratio of European beech (*Fagus sylvatica* L.). *Plants*. 2016; 5: 1010–1016. <https://doi.org/10.3390/plants5030038> PMID: 27618119
14. Uchytílová T, Krejza J, Veselá B, Holub P, Urban O, Horáček P, et al. Ultraviolet radiation modulates C: N stoichiometry and biomass allocation in *Fagus sylvatica* saplings cultivated under elevated CO<sub>2</sub> concentration. *Plant Physiol Biochem*. 2019; 134: 103–112. <https://doi.org/10.1016/j.plaphy.2018.07.038> PMID: 30097290
15. Ofori-Amanfo KK, Klem K, Veselá B, Holub P, Agyei T, Marek M V., et al. Interactive Effect of Elevated CO<sub>2</sub> and Reduced Summer Precipitation on Photosynthesis is Species-Specific: The Case Study with Soil-Planted Norway Spruce and Sessile Oak in a Mountainous Forest Plot. *Forests*. 2020; 12: 42. <https://doi.org/10.3390/f12010042>
16. Eamus D, Jarvis PG. The Direct Effects of Increase in the Global Atmospheric CO<sub>2</sub> Concentration on Natural and Commercial Temperate Trees and Forests. *Advances in Ecological Research*. 2004. pp. 1–58. [https://doi.org/10.1016/S0065-2504\(03\)34001-2](https://doi.org/10.1016/S0065-2504(03)34001-2)
17. Körner C. Plant CO<sub>2</sub> responses: An issue of definition, time and resource supply. *New Phytol*. 2006; 172: 393–411. <https://doi.org/10.1111/j.1469-8137.2006.01886.x> PMID: 17083672
18. Milanović S, Milenković I, Dobrosavljević J, Popović M, Solla A, Tomšovský M, et al. Growth rates of *lymantria dispar* larvae and *quercus robur* seedlings at elevated CO<sub>2</sub> concentration and phytophthora plurivora infection. *Forests*. 2020; 11: 1–14. <https://doi.org/10.3390/f11101059>

19. Jiang M, Medlyn BE, Drake JE, Duursma RA, Anderson IC, Barton CVM, et al. The fate of carbon in a mature forest under carbon dioxide enrichment. *Nature*. 2020; 580: 227–231. <https://doi.org/10.1038/s41586-020-2128-9> PMID: 32269351
20. Reich PB, Hungate BA, Luo Y. Carbon-nitrogen interactions in terrestrial ecosystems in response to rising atmospheric carbon dioxide. *Annu Rev Ecol Evol Syst*. 2006; 37: 611–636. <https://doi.org/10.1146/annurev.ecolsys.37.091305.110039>
21. Dieleman WIJ, Luysaert S, Rey A, De Angelis P, Barton CVM, Broadmeadow MSJ, et al. Soil [N] modulates soil C cycling in CO<sub>2</sub>-fumigated tree stands: A meta-analysis. *Plant, Cell Environ*. 2010; 33: 2001–2011. <https://doi.org/10.1111/j.1365-3040.2010.02201.x> PMID: 20573048
22. Norby RJ, Warren JM, Iversen CM, Medlyn BE, McMurtrie RE. CO<sub>2</sub> enhancement of forest productivity constrained by limited nitrogen availability. *Proc Natl Acad Sci U S A*. 2010. <https://doi.org/10.1073/pnas.1006463107> PMID: 20974944
23. Luo Y, Su B, Currie WS, Dukes JS, Finzi A, Hartwig U, et al. Progressive Nitrogen Limitation of Ecosystem Responses to Rising Atmospheric Carbon Dioxide. *Bioscience*. 2004; 54: 731.
24. Terrer C, Jackson RB, Prentice IC, Keenan TF, Kaiser C, Vicca S, et al. Nitrogen and phosphorus constrain the CO<sub>2</sub> fertilization of global plant biomass. *Nat Clim Chang*. 2019; 9: 684–689. <https://doi.org/10.1038/s41558-019-0545-2>
25. Kirschbaum MUF, Lambie SM. Re-analysis of plant CO<sub>2</sub> responses during the exponential growth phase: Interactions with light, temperature, nutrients and water availability. *Funct Plant Biol*. 2015; 42: 989–1000. <https://doi.org/10.1071/FP15103> PMID: 32480738
26. Yazaki K, Maruyama Y, Mori S, Koike T, Funada R. Effects of elevated carbon dioxide concentration on wood structure and formation in trees. *Plant Responses to Air Pollution and Global Change*. Tokyo: Springer Japan; 2005. pp. 89–97.
27. Wullschlegel SD, Tschaplinski TJ, Norby RJ. Plant water relations at elevated CO<sub>2</sub>—Implications for water-limited environments. *Plant, Cell Environ*. 2002; 25: 319–331. <https://doi.org/10.1046/j.1365-3040.2002.00796.x> PMID: 11841673
28. Watanabe Y, Tobita H, Kitao M, Maruyama Y, Choi DS, Sasa K, et al. Effects of elevated CO<sub>2</sub> and nitrogen on wood structure related to water transport in seedlings of two deciduous broad-leaved tree species. *Trees—Struct Funct*. 2008; 22: 403–411. <https://doi.org/10.1007/s00468-007-0201-8>
29. Ceulemans R, Jach ME, Van De Velde R, Lin JX, Stevens M. Elevated atmospheric CO<sub>2</sub> alters wood production, wood quality and wood strength of Scots pine (*Pinus sylvestris* L) after three years of enrichment. *Glob Chang Biol*. 2002; 8: 153–162. <https://doi.org/10.1046/j.1354-1013.2001.00461.x>
30. Domec JC, Smith DD, McCulloh KA. A synthesis of the effects of atmospheric carbon dioxide enrichment on plant hydraulics: implications for whole-plant water use efficiency and resistance to drought. *Plant Cell Environ*. 2017; 40: 921–937. <https://doi.org/10.1111/pce.12843> PMID: 27739596
31. Yazaki K, Funada R, Mori S, Maruyama Y, Abaimov AP, Kayama M, et al. Growth and annual ring structure of *Larix sibirica* grown at different carbon dioxide concentrations and nutrient supply rates. *Tree Physiol*. 2001; 21: 1223–1229. <https://doi.org/10.1093/treephys/21.16.1223> PMID: 11600344
32. Kaakinen S, Kostianen K, Ek F, Saranpää P, Kubiske ME, Sober J, et al. Stem wood properties of *Populus tremuloides*, *Betula papyrifera* and *Acer saccharum* saplings after 3 years of treatments to elevated carbon dioxide and ozone. *Glob Chang Biol*. 2004; 10: 1513–1525. <https://doi.org/10.1111/j.1365-2486.2004.00814.x>
33. Kostianen K, Jalkanen H, Kaakinen S, Saranpää P, Vapaavuori E. Wood properties of two silver birch clones exposed to elevated CO<sub>2</sub> and O<sub>3</sub>. *Glob Chang Biol*. 2006; 12: 1230–1240. <https://doi.org/10.1111/j.1365-2486.2006.01165.x>
34. Lotfiomran N, Fromm J, Luinstra GA. Effects of elevated CO<sub>2</sub> and different nutrient supplies on wood structure of European beech (*Fagus sylvatica*) and gray poplar (*Populus × canescens*). *IAWA J*. 2015; 36: 84–97. <https://doi.org/10.1163/22941932-00000087>
35. Atkinson CJ, Taylor JM. Effects of elevated CO<sub>2</sub> on stem growth, vessel area and hydraulic conductivity of oak and cherry seedlings. *New Phytol*. 1996; 133: 617–626. <https://doi.org/10.1111/j.1469-8137.1996.tb01930.x>
36. Watanabe Y, Satomura T, Sasa K, Funada R, Koike T. Differential anatomical responses to elevated CO<sub>2</sub> in saplings of four hardwood species. *Plant, Cell Environ*. 2010; 33: 1101–1111. <https://doi.org/10.1111/j.1365-3040.2010.02132.x> PMID: 20199624
37. Tyree ME, Zimmermann MH. *Xylem Structure and the Ascent of Sap (Second Edition)*. Springer Verlag. 2002.
38. Chave J, Coomes D, Jansen S, Lewis SL, Swenson NG, Zanne AE. Towards a worldwide wood economics spectrum. *Ecol Lett*. 2009; 12: 351–366. <https://doi.org/10.1111/j.1461-0248.2009.01285.x> PMID: 19243406

39. Ziemińska K, Butler DW, Gleason SM, Wright IJ, Westoby M. Fibre wall and lumen fractions drive wood density variation across 24 Australian angiosperms. *AoB Plants*. 2013; 5: 1–14. <https://doi.org/10.1093/aobpla/plt046>
40. Enquist BJ, West GB, Charnov EL, Brown JH. Allometric scaling of production and life-history variation in vascular plants. *Nature*. 1999; 401: 907–911. <https://doi.org/10.1038/44819>
41. Pretzsch H, Biber P, Schütze G, Kemmerer J, Uhl E. Wood density reduced while wood volume growth accelerated in Central European forests since 1870. *For Ecol Manage*. 2018; 429: 589–616. <https://doi.org/10.1016/j.foreco.2018.07.045>
42. Pietras J, Stojanović M, Knott R, Pokorný R. Oak sprouts grow better than seedlings under drought stress. *iForest—Biogeosciences For*. 2016; 009: e1–e7. <https://doi.org/10.3832/ifer1823-009>
43. McDowell NG, Allen CD, Anderson-Teixeira K, Aukema BH, Bond-Lamberty B, Chini L, et al. Pervasive shifts in forest dynamics in a changing world. *Science (80-)*. 2020; 368: eaaz9463. <https://doi.org/10.1126/science.aaz9463> PMID: 32467364
44. Allen CD, Macalady AK, Chenchouni H, Bachelet D, McDowell N, Vennetier M, et al. A global overview of drought and heat-induced tree mortality reveals emerging climate change risks for forests. *For Ecol Manage*. 2010; 259: 660–684. <https://doi.org/10.1016/j.foreco.2009.09.001>
45. Krejza J, Cienciala E, Světlík J, Bellan M, Noyer E, Horáček P, et al. Evidence of climate-induced stress of Norway spruce along elevation gradient preceding the current dieback in Central Europe. *Trees*. 2021; 35: 103–119. <https://doi.org/10.1007/s00468-020-02022-6>
46. Hanewinkel M, Cullmann DA, Schelhaas MJ, Nabuurs GJ, Zimmermann NE. Climate change may cause severe loss in the economic value of European forest land. *Nat Clim Chang*. 2013; 3: 203–207. <https://doi.org/10.1038/nclimate1687>
47. Kohler M, Pyttel P, Kuehne C, Modrow T, Bauhus J. On the knowns and unknowns of natural regeneration of silviculturally managed sessile oak (*Quercus petraea* (Matt.) Liebl.) forests—a literature review. *Ann For Sci*. 2020; 77: 1–19. <https://doi.org/10.1007/s13595-020-00998-2>
48. Mölder A, Meyer P, Nagel RV. Integrative management to sustain biodiversity and ecological continuity in Central European temperate oak (*Quercus robur*, *Q. petraea*) forests: An overview. *For Ecol Manage*. 2019; 437: 324–339. <https://doi.org/10.1016/j.foreco.2019.01.006>
49. Cochard H, Bréda N, Granier A. Whole tree hydraulic conductance and water loss regulation in *Quercus* during drought: evidence for stomatal control of embolism? *Ann des Sci For*. 1996; 53: 197–206. <https://doi.org/10.1051/forest:19960203>
50. Stojanović M, Szatniewska J, Kyselová I, Pokorný R, Čáter M. Transpiration and water potential of young *Quercus petraea* (M.) Liebl. coppice sprouts and seedlings during favourable and drought conditions. *J For Sci*. 2017; 63: 313–323. <https://doi.org/10.17221/36/2017-JFS>
51. Nölte A, Yousefpour R, Hanewinkel M. Changes in sessile oak (*Quercus petraea*) productivity under climate change by improved leaf phenology in the 3-PG model. *Ecol Modell*. 2020; 438: 109285. <https://doi.org/10.1016/j.ecolmodel.2020.109285>
52. Kunz J, Löffler G, Bauhus J. Minor European broadleaved tree species are more drought-tolerant than *Fagus sylvatica* but not more tolerant than *Quercus petraea*. *For Ecol Manage*. 2018; 414: 15–27. <https://doi.org/10.1016/j.foreco.2018.02.016>
53. Bergès L, Nepveu G, Franc A. Effects of ecological factors on radial growth and wood density components of sessile oak (*Quercus petraea* Liebl.) in Northern France. *For Ecol Manage*. 2008; 255: 567–579. <https://doi.org/10.1016/j.foreco.2007.09.027>
54. Lauriks F, Salomón RL, De Roo L, Steppe K. Leaf and tree responses of young European aspen trees to elevated atmospheric CO<sub>2</sub> concentration vary over the season. *Tree Physiol*. 2021; 1–28.
55. Cha S, Chae HM, Lee SH, Shim JK. Effect of elevated atmospheric CO<sub>2</sub> concentration on growth and leaf litter decomposition of *Quercus acutissima* and *Fraxinus rhynchophylla*. *PLoS One*. 2017; 12: 14–16. <https://doi.org/10.1371/journal.pone.0171197> PMID: 28182638
56. Urban O, Janouš D, Pokorný R, Markova I, Pavelka M, Fojtík Z, et al. Glass domes with adjustable windows: A novel technique for exposing juvenile forest stands to elevated CO<sub>2</sub> concentration. *Photosynthetica*. 2001. pp. 395–401. <https://doi.org/10.1023/A:1015134427592>
57. Williamson GB, Wiemann MC. Measuring wood specific gravity . . . correctly. *Am J Bot*. 2010; 97: 519–524. <https://doi.org/10.3732/ajb.0900243> PMID: 21622413
58. Rossi S, Anfodillo T, Menardi R. Trephor: A New Tool for Sampling Microcores from tree stems. *IAWA J*. 2006; 27: 89–97. <https://doi.org/10.1163/22941932-90000139>
59. Fajstavr M, Giagli K, Vavrčik H, Gryc V, Horáček P, Urban J. The cambial response of Scots pine trees to girdling and water stress. *IAWA J*. 2020; 41: 159–185. <https://doi.org/10.1163/22941932-bja10004>
60. Schneider CA, Rasband WS, Eliceiri KW. NIH Image to ImageJ: 25 years of image analysis. *Nat Methods*. 2012; 9: 671–675. <https://doi.org/10.1038/nmeth.2089> PMID: 22930834

61. Fonti P, Heller O, Cherubini P, Rigling A, Arend M. Wood anatomical responses of oak saplings exposed to air warming and soil drought. *Plant Biol.* 2013; 15: 210–219. <https://doi.org/10.1111/j.1438-8677.2012.00599.x> PMID: 22612857
62. Tyree MT, Ewers FW. The hydraulic architecture of trees and other woody plants. *New Phytol.* 1991; 119: 345–360. <https://doi.org/10.1111/j.1469-8137.1991.tb00035.x>
63. Noyer E, Lachenbruch B, Dlouhá J, Collet C, Ruelle J, Ningre F, et al. Xylem traits in European beech (*Fagus sylvatica* L.) display a large plasticity in response to canopy release. *Ann For Sci.* 2017; 74: 46. <https://doi.org/10.1007/s13595-017-0634-1>
64. Stojanović M, Sánchez-Salguero R, Levanič T, Szatniewska J, Pokorný R, Linares JC. Forecasting tree growth in coppiced and high forests in the Czech Republic. The legacy of management drives the coming *Quercus petraea* climate responses. *For Ecol Manage.* 2017; 405: 56–68. <https://doi.org/10.1016/j.foreco.2017.09.021>
65. Carlquist S. Ecological factors in wood evolution: a floristic approach. *Am J Bot.* 1977; 64: 887–896. <https://doi.org/10.1002/j.1537-2197.1977.tb11932.x>
66. Copini P, Vergeldt FJ, Fonti P, Sass-Klaassen U, den Ouden J, Sterck F, et al. Magnetic resonance imaging suggests functional role of previous year vessels and fibres in ring-porous sap flow resumption. Steppe K, editor. *Tree Physiol.* 2019; 39: 1009–1018. <https://doi.org/10.1093/treephys/tpz019> PMID: 30896019
67. Taneda H, Sperry JS. A case-study of water transport in co-occurring ring- versus diffuse-porous trees: Contrasts in water-status, conducting capacity, cavitation and vessel refilling. *Tree Physiol.* 2008; 28: 1641–1651. <https://doi.org/10.1093/treephys/28.11.1641> PMID: 18765369
68. Sevanto S, Michele Holbrook N, Ball MC. Freeze/thaw-induced embolism: Probability of critical bubble formation depends on speed of ice formation. *Front Plant Sci.* 2012; 3: 1–12.
69. Wood SN. Generalized additive models: An introduction with R, second edition. *Generalized Additive Models: An Introduction with R, Second Edition.* 2017.
70. Kirschbaum MUF. Direct and indirect climate change effects on photosynthesis and transpiration. *Plant Biol.* 2004; 6: 242–253. <https://doi.org/10.1055/s-2004-820883> PMID: 15143433
71. Saxe H, Ellsworth DS, Heath J. Tree and forest functioning in an enriched CO<sub>2</sub> atmosphere. *New Phytol.* 1998; 139: 395–436. <https://doi.org/10.1046/j.1469-8137.1998.00221.x>
72. Steppe K, Sterck F, Deslauriers A. Diel growth dynamics in tree stems: Linking anatomy and ecophysiology. *Trends Plant Sci.* 2015; 20: 335–343. <https://doi.org/10.1016/j.tplants.2015.03.015> PMID: 25911419
73. Pantin F, Simonneau T, Muller B. Coming of leaf age: Control of growth by hydraulics and metabolics during leaf ontogeny. *New Phytol.* 2012; 196: 349–366. <https://doi.org/10.1111/j.1469-8137.2012.04273.x> PMID: 22924516
74. Körner C. Carbon limitation in trees. *J Ecol.* 2003; 91: 4–17. <https://doi.org/10.1046/j.1365-2745.2003.00742.x>
75. Muller B, Pantin F, Génard M, Turc O, Freixes S, Piques M, et al. Water deficits uncouple growth from photosynthesis, increase C content, and modify the relationships between C and growth in sink organs. *J Exp Bot.* 2011; 62: 1715–1729. <https://doi.org/10.1093/jxb/erq438> PMID: 21239376
76. Peters RL, Steppe K, Cuny HE, De Pauw DJW, Frank DC, Schaub M, et al. Turgor—a limiting factor for radial growth in mature conifers along an elevational gradient. *New Phytol.* 2020. <https://doi.org/10.1111/nph.16872> PMID: 32790914
77. Bin Luo Z, Langenfeld-Heyser R, Calfapietra C, Polle A. Influence of free air CO<sub>2</sub> enrichment (EUROFACE) and nitrogen fertilisation on the anatomy of juvenile wood of three poplar species after coppicing. *Trees—Struct Funct.* 2005; 19: 109–118. <https://doi.org/10.1007/s00468-004-0369-0>
78. Rao R V., Aebischer DP, Denne MP. Latewood density in relation to wood fibre diameter, wall thickness, and fibre and vessel percentages in *Quercus robur* L. *IAWA J.* 1997; 18: 127–138. <https://doi.org/10.1163/22941932-90001474>
79. Leal S, Sousa VB, Knapic S, Louzada JL, Pereira H. Vessel size and number are contributors to define wood density in cork oak. *Eur J For Res.* 2011; 130: 1023–1029. <https://doi.org/10.1007/s10342-011-0487-3>
80. Norby RJ, O'Neill EG, Luxmoore RJ. Effects of Atmospheric CO<sub>2</sub> Enrichment on the Growth and Mineral Nutrition of *Quercus alba* Seedlings in Nutrient-Poor Soil. *Plant Physiol.* 1986; 82: 83–89. <https://doi.org/10.1104/pp.82.1.83> PMID: 16665028
81. Stitt M, Krapp A. The interaction between elevated carbon dioxide and nitrogen nutrition: the physiological and molecular background. 1999; 583–621. <https://doi.org/10.1046/j.1365-3040.1999.00386.x>
82. Rolo V, Andivia E, Pokorný R. Response of *Fagus sylvatica* and *Picea abies* to the interactive effect of neighbor identity and enhanced CO<sub>2</sub> levels. *Trees—Struct Funct.* 2015; 29: 1459–1469. <https://doi.org/10.1007/s00468-015-1225-0>



83. Hacke UG, Sperry JS, Pittermann J. Efficiency Versus Safety Tradeoffs for Water Conduction in Angiosperm Vessels Versus Gymnosperm Tracheids. *Vascular Transport in Plants*. Elsevier; 2005. pp. 333–353. <https://doi.org/10.1016/B978-012088457-5/50018-6>
84. Levanic T, Cater M, McDowell NG. Associations between growth, wood anatomy, carbon isotope discrimination and mortality in a *Quercus robur* forest. *Tree Physiol*. 2011; 31: 298–308. <https://doi.org/10.1093/treephys/tpq111> PMID: 21367747
85. Niklas KJ, Spatz H. Worldwide correlations of mechanical properties and green wood density. *Am J Bot*. 2010; 97: 1587–1594. <https://doi.org/10.3732/ajb.1000150> PMID: 21616793
86. Larjavaara M, Muller-Landau HC. Rethinking the value of high wood density. *Funct Ecol*. 2010; 24: 701–705. <https://doi.org/10.1111/j.1365-2435.2010.01698.x>
87. Badel E, Ewers FW, Cochard H, Telewski FW. Acclimation of mechanical and hydraulic functions in trees: impact of the thigmomorphogenetic process. *Front Plant Sci*. 2015; 6: 1–12.
88. Fournier M, Dlouhá J, Jaouen G, Almeras T. Integrative biomechanics for tree ecology: beyond wood density and strength. *J Exp Bot*. 2013; 64: 4793–4815. <https://doi.org/10.1093/jxb/ert279> PMID: 24014867
89. Schelhaas MJ, Nabuurs GJ, Schuck A. Natural disturbances in the European forests in the 19th and 20th centuries. *Glob Chang Biol*. 2003; 9: 1620–1633. <https://doi.org/10.1046/j.1365-2486.2003.00684.x>
90. Zobel BJ, Sprague JR. Predictions of Mature and Total Tree Wood Properties from Juvenile Wood. *Juvenile Wood in Forest Trees*. 1998. pp. 173–187. [https://doi.org/10.1007/978-3-642-72126-7\\_6](https://doi.org/10.1007/978-3-642-72126-7_6)
91. Brienens RJW, Caldwell L, Duchesne L, Voelker S, Barichivich J, Baliva M, et al. Forest carbon sink neutralized by pervasive growth-lifespan trade-offs. *Nat Commun*. 2020; 11: 4241. <https://doi.org/10.1038/s41467-020-17966-z> PMID: 32901006